1987

Isostatic Compensation and Conduit Structures of Western Pacific Seamounts: Results of Three-Dimensional Gravity Modeling

James N. Kellogg
University of South Carolina - Columbia, kellogg@geol.sc.edu

Bruce S. Wedgeworth

Jeffrey T. Freymueller

Publication Info

Published in *Geophysical Monograph Series*, ed. B. H. Keating, P. Fryer, R. Batiza, G. W. Boehlert, Volume 43, 1987, pages 85-96.
Kellogg, J. N., Wedgeworth, B. S., & Freymueller, J. T. (1987). Isostatic compensation and conduit structures of Western Pacific seamounts: Results of three-dimensional gravity modeling. *Seamounts, Islands, and Atolls, 43*, 85-96.

ISOSTATIC COMPENSATION AND CONDUIT STRUCTURES OF WESTERN PACIFIC SEAMOUNTS: RESULTS OF THREE-DIMENSIONAL GRAVITY MODELING

J. N. Kellogg[1], B. S. Wedgeworth[2], and J. Freymueller[1]

Hawaii Institute of Geophysics, Honolulu, Hawaii 96822

Abstract. Detailed three-dimensional polygonal prism models of two large western Pacific seamounts show that the 135 mgal difference in the observed sea surface gravity over the two can be best explained by similar mean densities (2.6 g/cm^3) and crustal thickening under one seamount (Airy isostatic compensation). Observed - calculated residuals are further reduced by including dense (2.9 g/cm^3) vertical feeder pipes or volcanic conduits in the models. Dense conduits or fracture zones 5 to 17 km in diameter are located under many, if not all, craters on volcanic islands and seamounts. Results from the detailed seamount studies can be generalized using exact expressions for the on-axis vertical component of gravity for cones or frustrums of cones. Seamount isostatic compensation levels can then be rapidly estimated by iteratively inverting the on-axis gravity. The estimation algorithm is independent of mechanical assumptions regarding oceanic lithosphere and is particularly useful for the rapid evaluation of large data sets. The results and associated uncertainties are comparable to those of the detailed three-dimensional models and frequency domain studies. As predicted by cooling plate models, the estimated Airy (local) compensation levels μ for seamounts are inversely proportional to the root of the seafloor age at the time of loading t: $\mu(\%) = 68 - 5.6t^{1/2}$. A map of depth-corrected on-axis gravity values for western Pacific seamounts indicates that seamounts with similar μ values tend to form clusters.

Introduction

The marine gravitational field provides important information regarding bathymetry and the structure of the oceanic crust and upper mantle. The Seasat radar altimeter generated a considerable amount of new information about the short-wavelength (30-400 km) character of the oceanic geoid. A major contribution to the marine geoid is made by seafloor bathymetry, because of the large density contrast at the rock-water interface. Attempts have therefore been made to use satellite altimeter data to predict bathymetry (e.g., Lazarewicz and Schwank, 1982; Dixon et al., 1983). Such a tool would be especially useful in the South and West Pacific where ship crossings are rare. Large areas are known to no better than 100-km resolution, and many first-order features such as seamount chains and fracture zones may be undetected. At the present time, however, successful bathymetric predictions from the Seasat altimeter data have been prevented by (1) uncertainties regarding the distances between the satellite tracks and the axes of bathymetric features and (2) large observed variations in the short- wavelength gravity-depth function.

The first obstacle, estimating off-track distance to a bathymetric feature, can be diminished as the GEOSAT, NROSS, TOPEX, ERS-1, and GRM satellites become operational, thereby substantially increasing the spatial density of sea-surface observations.

Our paper addresses the second obstacle to successful bathymetric predictions from altimeter data: the large variation in the short-wavelength gravity-depth function, that relates maximum sea-surface gravity anomalies and minimum depth to bathymetric features (30-400 km) in wavelength. For example, sea surface free-air gravity anomalies over seamounts of the same size and depth may vary by up to 200 mgal or over 4 meters on the geoid. Vogt et al. (1984) showed that the Seasat radar altimetry and seafloor topography over Bermuda and Gregg Seamount could not be described adequately by a single transfer function. Dixon et al (1983) and Watts and Ribe (1984) related the variations in amplitude of marine geoid anomalies over seamounts to different effective elastic thicknesses of the flexed lithosphere beneath the seamounts. The effective elastic thicknesses are related to the tectonic settings of the seamounts, that is, whether they formed on or near a mid-oceanic ridge crest or off-ridge. Bathymetric prediction from altimeter data directly is therefore difficult unless a priori constraints on the tectonic settings of the seamounts are available. In this paper we will present gravity data from the Mid-Pacific Mountains and the Marshall Island Group indicating that seamounts in lines or spatial clusters have similar gravity-depth relationships and presumably similar tectonic origins.

The gravitational field is the vertical gradient of the potential, and is therefore even more sensitive to nearby shallow mass anomalies than the geoid. The sea surface gravity field over well surveyed seamounts is known better and contains more short wavelength information than the Seasat derived geoid. Previous studies have been limited to gravity anomalies over a relatively few seamounts and oceanic islands (e.g., Watts and Ribe, 1984; Kellogg and Ogujiofor, 1985; Freedman and Parsons, 1986). In this paper, pertinent gravity and bathymetric data are presented together for most of the well-surveyed seamounts and islands in the western Pacific, permitting evaluation of the variations in the short wavelength (30-400 km) gravity-depth function for the western Pacific. We show with three dimensional models that the observed variations in the gravity-depth function can be explained by varying degrees of local Airy isostatic compensation. High resolution surface gravity data permit the quantification of small wavelength (< 30 km) seamount features such as conduit zones. In this paper we estimate the densities and geometries of seamount conduits from gravity and seismic refraction studies and infer their compositions from published petrologic studies. We present a simple iterative in-

[1]Now at Department of Geological Sciences, University of South Carolina, Columbia, South Carolina

[2]Now at Harding Lawson Associates, Honolulu, Hawaii

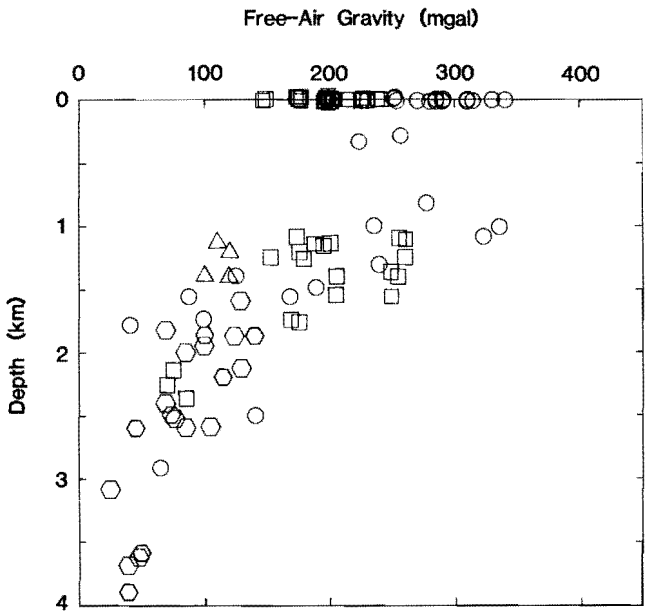

Fig. 1. Maximum free-air gravity anomalies as a function of minimum depths to the tops of 59 seamounts in the western Pacific. For 38 islands and atolls in the western Pacific, maximum Bouguer anomalies (density = 2.3 g/cm^3) are plotted at sea level. The Mid-Pacific Mountains are shown as triangles, the Marshall Islands Group and East Mariana Basin Seamounts as squares, the Musicians Seamounts as hexagons, and the Magellan Seamounts, Hawaiian-Emperor Ridge, and Kiribati and Caroline Islands as circles.

verse method to rapidly estimate the degree of isostatic compensation for large numbers of well-surveyed seamounts. Finally, we discuss the implications of the regional clustering of seamounts with similar isostatic compensation levels for bathymetric prediction from satellite altimetry data.

Observed Gravity-Depth Function

The short wavelength (< 400 km) marine gravity field is a function of seafloor topography and lateral density variations in the crust and upper mantle. Sea surface gravity fields observed over seamounts are related to their sizes, shapes, minimum depths, seafloor depths, edifice densities, and density variations in the lithosphere beneath the seamounts. Understanding the relationship between the gravity field and the minimum depths to the tops of seamounts is needed to accurately predict seamount depths from satellite altimetry and is therefore a matter of great importance for submarine navigation and mineral exploration in the many parts of the world's oceans where bathymetric coverage by surface ships is inadequate.

Maximum free-air gravity anomalies are plotted in Figure 1 as a function of minimum depths to the tops of 59 seamounts in the Western Pacific. For 38 islands and atolls in the Western Pacific, maximum Bouguer anomalies ($\rho = 2.3$ g/cm^3) are plotted at sea level. Only well surveyed edifices are included to ensure that the gravity anomalies are not underestimated.

Not surprisingly, the data indicate a general inverse correlation between depth and gravity anomalies. A linear estimate for the mean gravity-depth relation is $z = -16g_z + 3800$ m where z is the minimum depth (m) to the top of the seamount and g_z is the maximum gravity anomaly (mgal) observed at the sea surface. There is considerable scatter about the mean however, thus permitting an estimate of the uncertainties in predicting bathymetry directly from gravity or geoid data alone in the Western Pacific. For example, although Sio Guyot, a large seamount in the western Mid-Pacific Mountains (Kellogg and Ogujiofor, 1985), is larger and shallower (z = 1130 m) than Ita Mai Tai in the East Mariana Basin (z = 1402 m) (Wedgeworth, 1985; Wedgeworth and Kellogg, this volume), it has a maximum free-air gravity anomaly (120 mgal) that is 135 mgal lower than that of Ita Mai Tai (255 mgal) (Figure 2). If we had attempted to predict the minimum depth to Sio Guyot from gravity data alone using our mean gravity depth relation for the western Pacific, $z = -16(120) + 3800 =$ 1880 m, or 750 m too deep. Inserting the gravity data for Ita Mai Tai in the same formula gives a value of $z = -16(255) + 3800 = -280$ m, or 280 m above sea level, or 1682 m too high. From Figure 1 we see that gravity values for edifices at the same depth in the Western Pacific vary up to 200 mgal (or over 4 m on the geoid). Thus, with no other constraints, the uncertainties involved in depth predictions for Western Pacific seamounts from gravity data alone are as great as ± 1600 m. This large uncertainty range is unsatisfactory, so we will offer an explanation based on three-dimensional gravity modeling and present possible constraints for depth predictions caused by clustering of seamounts with similar gravity-depth ratios.

Three-Dimensional Models of Sio and Ita Mai Tai Guyots

To better understand the wide variations in gravity fields over seamounts, we modeled the gravity fields of Sio Guyot and Ita Mai Tai Guyot. Sio Guyot consists of two flat-topped summits among a cluster of six large guyots surmounting a broad basement swell or plateau (Nemoto and Kroenke, 1985). The Mid-Pacific Mountains extend over 2000 km eastward almost to the midpoint of the Hawaiian Ridge. The northern summit area of Sio Guyot (2820 km^2), lying between 1130 and 1500 m below sea level, is much greater than the exposed summit area of the island of Oahu, Hawaii (1650 km^2). At a depth of about 3400 m the 8° slopes of the guyot merge with the broad plateau that slopes gradually to 5500 m abyssal depths. Ita Mai Tai Guyot is smaller, subconical in shape, and has no underlying plateau. The flat-topped summit lies between 1400 and 2200 m and covers an area of about 1500 km^2.

We found empirically that to limit model density uncertainties to ± 0.1 g/cm^3, the gravity field must be calculated with less than 6% error. A three-dimensional method was used because the two-dimensional method (assuming that polygonal prisms extend infinitely perpendicular to the profile) overcorrects the gravity effect by 18% over the apex of a conical seamount with a 10° slope (Rose and Bowman, 1974). The relatively few published three-dimensional models for seamounts include Harrison and Brisbin (1959), Le Pichon and Talwani (1964), Watts et al. (1975), and Sager et al. (1982). The bathymetry for Sio and Ita Mai Tai guyots was approximated with 33 and 11 vertical-sided polygonal prisms respectively (Figures 3 and 4). The observed gravity fields were digitized for 980 grid points each at 9 and 5 km intervals.

Linear least-squares inversion of observed gravity anomalies can sometimes be used to help determine the average density of seamounts. This technique is fundamentally the same as the density-profiling method (Nettleton, 1939). The main assumption is that the wavelength of any subsurface anomalous distribution of mass must be much shorter or much longer than the dimensions of the bathymetric feature being studied. Lewis and Dorman (1970) pointed out that this method is successful only for topography with wavelengths much shorter than those of gravity anomalies produced by regional isostatic compensation. This technique is not valid for a seamount if it has a local gravity "root" or a large magma chamber (Le Pichon and Talwani, 1964). Inversion of the gravity field over Ita Mai Tai produced a calculated mean density of 2.59 g/cm^3, but inversion of the field

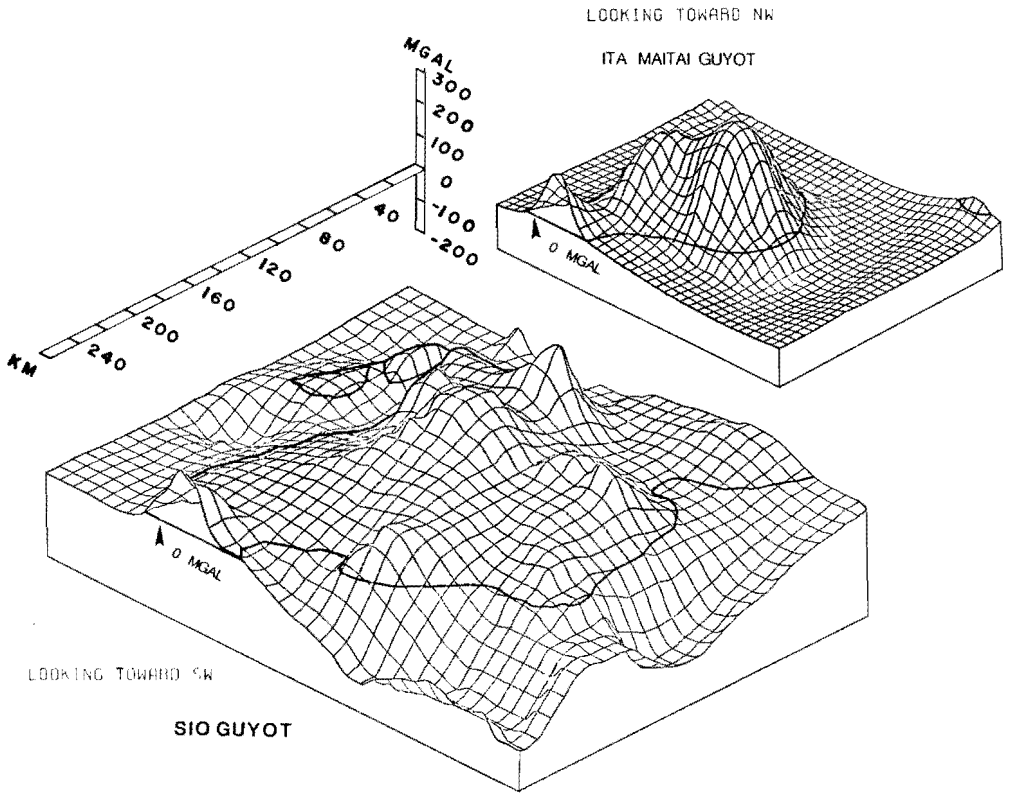

Fig. 2. Free-air gravity anomalies over Sio and Ita Mai Tai Guyots. Although Sio Guyot, a large seamount in the western Mid-Pacific Mountains, is larger and shallower than Ita Mai Tai Guyot in the East Mariana Basin, it has a maximum gravity anomaly 135 mgal lower than that of Ita Mai Tai. Seamount locations are shown in Figure 15.

over Sio Guyot resulted in an impossible low value of 1.95 g/cm^3. Le Pichon and Talwani (1964) obtained a similar density of 1.9 g/cm^3 for a seamount near the Mid-Atlantic Ridge, which they also rejected as erroneous. The fact that the positive gravity anomaly over Sio Guyot has a low amplitude and is flanked by negative anomalies suggests that there may be a broad zone of low density below the plateau with about the same wavelength as the plateau itself. Therefore, for realistic models we must rely on direct measurements of rock densities and seismic refraction velocities from other seamounts.

Measurements of seamount and oceanic island rock densities by Harrison and Brisbin (1959), Nayudu (1962), Kinoshita et al. (1963), Strange et al. (1965), and Manghnani and Woollard (1965) are summarized by Kellogg and Ogujiofor (1985). The measurements suggest that the mean densities of all seamounts lie between 2.3 and 2.9 g/cm^3.

Seismic compressional (P-wave) velocities can also be used to estimate density (Nafe and Drake, 1963). Seismic velocities have been measured for a seamount north of Madeira and two peaks in the Mid-Atlantic Rift Valley (Laughton et al., 1960), Cruiser Seamount (Le Pichon and Talwani, 1964), Bermuda (Officer et al., 1952), Bikini and Kwajalein (Raitt, 1954), the flanks of the Hawaiian Ridge north of Maui (Shor and Pollard, 1964), Oahu (Furumoto and Woollard, 1965; Furumoto et al., 1965; Watts et al., 1985), Tahiti and Rangiroa (Talandier and Okal, in press). The refraction data support the occurrence of a layer of 3.6 to 4.6 km/sec material over basaltic rock of a velocity 5.2 to 6.2 km/sec within the seamount. From the Nafe-Drake curve, these velocities correspond to densities of about 2.30 to 2.50 g/cm^3 and 2.60 to 2.75 g/cm^3, respectively.

The density obtained by inverting the gravity field for Ita Mai Tai (2.59 g/cm^3) is well within the range both of directly measured values and inferred values from seismic compressional velocities for the other seamounts. The density obtained by inverting the data for Sio Guyot (1.95 g/cm^3), however, is too low. We therefore, used realistic densities of 2.5 to 2.7 g/cm^3 for the basal swell or plateau, 2.9 g/cm^3 for the oceanic crust, and 3.4 g/cm^3 for the upper mantle (Figure 5, Kellogg and Ogujiofor, 1985). The first model was "uncompensated" (i.e., the excess mass of the guyot was not balanced by a mass deficit or local "root" directly beneath the guyot) and a uniform crystalline crustal thickness of 6.3 km was assumed (Woollard, 1975). The gravity anomalies of the polygonal prisms were calculated according to the method of Plouff (1976). Correlation between observed and calculated values was poor, along-track residual anomalies were as high as 100 mgal over the abyssal sea floor and as low as -80 mgal over Sio Guyot (Figure 5). From seismic refraction and wide-angle reflection surveys the crust is known to bend and thicken under the Hawaiian Ridge (Shor and Pollard, 1964; Furumoto et al., 1968; Suyenaga, 1979; Zucca et al., 1982; Watts et al., 1985) and under Rangiroa in the Tuamotu Islands (Talandier and Okal, in press), so to account for the apparent mass deficiency beneath Sio Guyot, "compensated" models with a thicker crust were tested. A cross section of the best fitting (minimum along-track residual anomalies) model is shown in Figure 5. In this model, the excess mass of the seamount is 70% "compensated locally" (i.e., balanced by a mass deficit directly beneath the seamount). If we assume that regional compensation is 100%, then 70% is the fraction of the compensation that is purely local. The residual gravity values (observed minus calculated) were

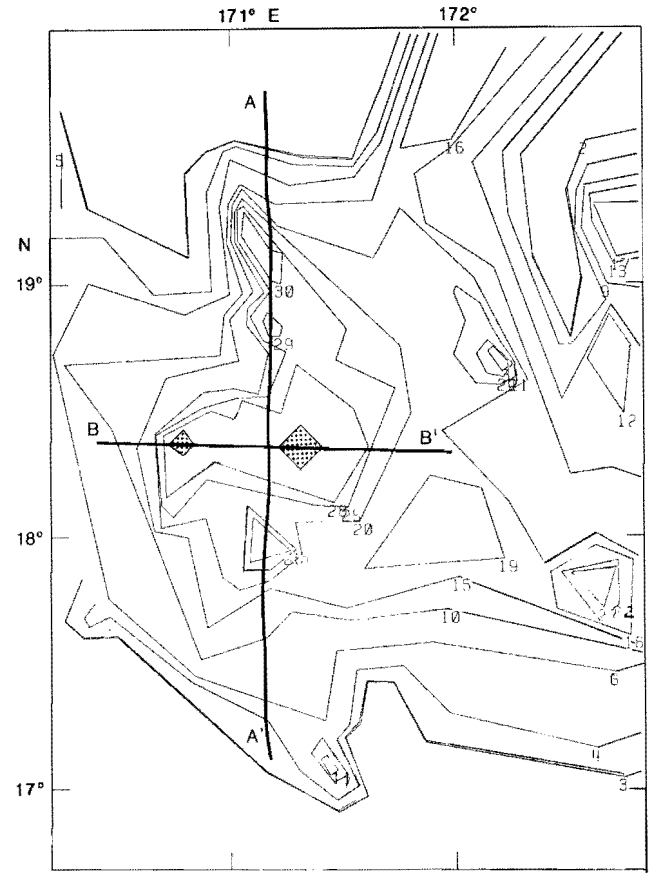

Fig. 3. Plan view of polygonal prisms used to approximate the bathymetry of Sio Guyot (after Kellogg and Ogujiofor, 1985).

low, less than 10 mgal along most of the ship track. The low density root in the compensated model accounts for the low amplitude of the positive gravity anomalies over the guyot as well as the negative anomalies flanking the plateau. In the best-fitting model, the crust underlying the guyot is 16 km thick and extends to a depth of 22 km. *An uncertainty in the density contrast at the crust-mantle boundary* of $\pm$ 0.1 g/cm^3 would result in a Moho depth uncertainty of $\pm$ 2 km.

Calculated gravity anomalies assuming a homogeneous edifice density of 2.59 g/cm^3 fit the observed gravity field over Ita Mai Tai fairly well. To explain the gravity lows flanking the seamount, however, the model was corrected for the low density clays and volcaniclastic debris in the basins to the north and east of the seamount (Figure 6; Wedgeworth, 1985; Wedgeworth and Kellogg, this volume). Sediment densities and thicknesses were derived from velocity measurements in the drilling record of DSDP Site 585 (Scientific Party, Leg 89, 1983) as well as HIG and DSDP Leg 89 seismic reflection records. To further reduce residual gravity anomalies, the crust was thickened just 1.5 km in the model. The large difference in the amplitudes of the observed gravity fields over the two seamounts (135 mgal) can be explained by varying levels of local isostatic compensation, with Sio Guyot 70% compensated and Ita Mai Tai only 8% compensated.

Eruptive Centers or Conduits

Although different depths to the crust-mantle boundary can explain the longer wavelength gravity anomalies over Sio and Ita Mai Tai guyots, they do not account for two short wavelength positive anomalies over Sio Guyot and one over Ita Mai Tai. To explain these anomalies, quadrilateral prisms of densities 2.8 to 3.0 g/cm^3 or 0.3 to 0.5 g/cm^3 higher than the surrounding layers were added to the models (Figures 6 and 7). The crustal structure shown along the cross-section B-B' (Figure 7) has a negligible effect on the short-wavelength anomalies.

The density models shown in Figures 6 and 7 could be explained by dense eruptive centers or conduits. Kroenke et al. (1966) modeled the positive gravity anomaly observed over Midway Atoll as the result of a volcanic conduit with a density of 3.2 g/cm^3 at a depth of 2 km. A similar volcanic center has been studied in the Koolau caldera on the island of Oahu (Strange et al., 1965), where nephelinite had a measured density of 3.0 g/cm^3 and seismic velocities were 6.1 km/sec within 1 km of the surface and 7.7 km/sec at a depth of 4 km (Furumoto et al., 1965). The observed positive gravity anomaly over the Koolau Volcano was matched by a calculated anomaly for a wide volcanic pipe with a density of 2.9 g/cm^3 within 2 km of the surface and 3.2 g/cm^3 at greater depths (Strange et al., 1965). The presence of abundant dunite xenoliths in olivine nephelinite vents of the Koolau crater led Sen (1983) to speculate that the dense Koolau plug represents deformed cumulate dunites and Fe-rich spinel pyroxenites frozen in the conduit. Primary CO_2 fluid inclusions in the dunite olivines suggest a maximum pressure of about 5 kbar (15 km depth) for the formation of these dunites (Roedder, 1965).

Conduit diameters estimated from gravity data are approximately 4 to 10 km for seven seamounts along the Bonin Arc (Ishihara, this volume), 5 km for Midway Atoll (Kroenke et al., 1966), 9 and 14 km for Sio Guyot (Figure 7), 17 km for Ita Mai Tai Guyot (Figure 6), and 7 to 17 km for Koolau Volcano on Oahu (Strange et al., 1965). Dense volcanic cores have also been recognized from gravity surveys of Manahiki Atoll, and Mangaia, Mauke, Mitiaro, Rarotonga, Atiu, Manuae, and Nassau Islands in the Cook Group (Robertson, 1967; 1970), Tutuila, Ofu, Olosega, and Tau Islands in American Samoa and Moorea Island in French Polynesia (Machesky, 1965). In Tahiti, positive gravity anomalies are centered over two exposed caldera cores of nepheline monzonites, theralites, and essexites (Williams,

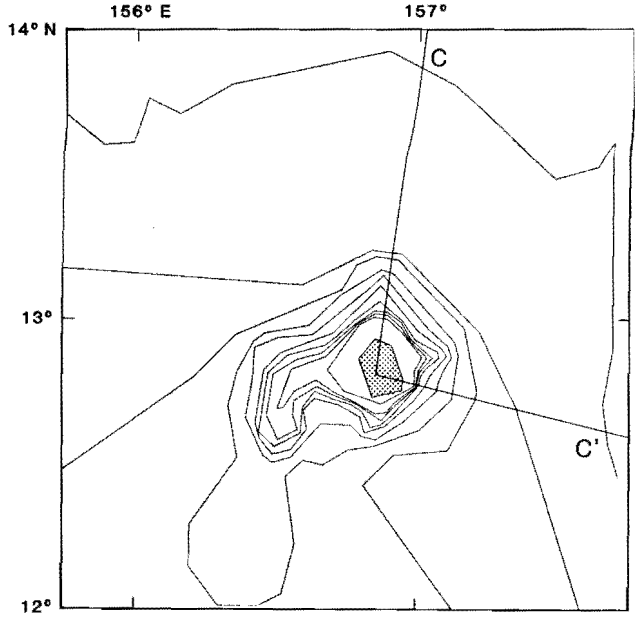

Fig. 4. Polygonal prism model of Ita Mai Tai Guyot (after Wedgeworth and Kellogg, this volume).

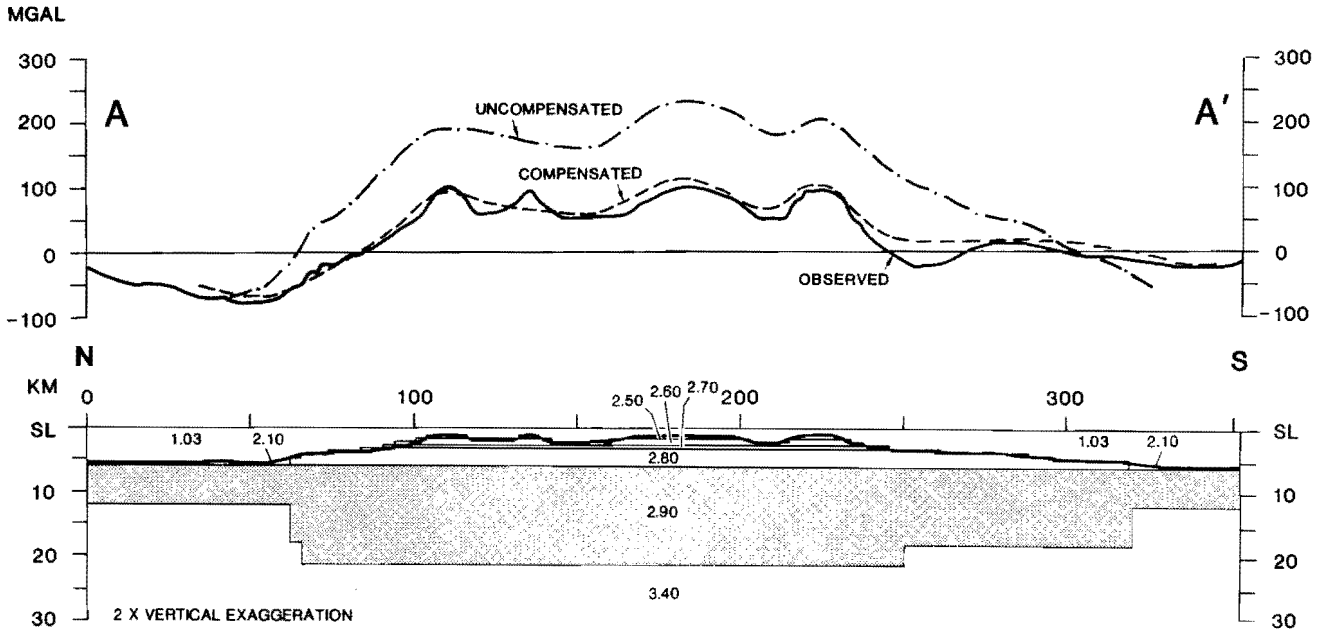

Fig. 5. Cross-section of the compensated density model for Sio Guyot showing observed and calculated free-air gravity anomalies for compensated and uncompensated models (Kellogg and Ogujiofor, 1985). Location shown in Figure 3.

1933; Machesky, 1965). These studies suggest that dense feeder pipes or volcanic conduits may be more common on volcanic islands and seamounts than previously thought, and may in fact be the norm.

Large positive gravity anomalies are located over active Kilauea and Mauna Loa craters on the island of Hawaii. On the basis of seismic activity and tilt data, Eaton (1962) has estimated that magma originates at a depth of 60 km below sea level and rises through a conduit to a magma chamber a few kilometers below the surface, where it remains until sufficient pressure is built up to cause an eruption. Hypocenters of earthquakes induced by the movement of magma define the fracture zone or conduit beneath Kilauea as elliptical in horizontal section with axial dimensions of 1 to 6 km (Ryan et al., 1981). Magma is then intruded from shallow magma chambers through dikes into the summit and east rift zone. P-wave traveltimes, positive gravity anomalies, and triangulation surveys suggest that the rift zone is spreading in response to magma intrusion (Swanson et al., 1976) forming a dense wedge of dikes and submarine pillow basalts covered by hyaloclastic products and subareal basalt flows (Hill and Zucca, 1987).

Generalized Three Dimensional Seamount Gravity Models

To determine whether varying local isostatic compensation levels could also explain the scatter in the gravity-depth function forother seamounts and islands in the western Pacific, we developed three-dimensional models for general cases.

The shapes of seamounts and islands were approximated with vertical-sided polygonal prisms in the form of right circular cones (conical seamounts) and frustrums of cones (guyots and islands) (Figures 8 and 9). The height to basal radius ratios $\xi = h/a_1$, (Figure 10) and the flatness ratios $f = a_2/a_1$ were estimated from wide-beam and side-scan bathymetric surveys of 63 seamounts and islands in the western Pacific. The mean height to basal radius ratio $\xi = 0.187 \pm 0.056$ was obtained by equally weighting the 28 estimates for seamounts with basal radius $a_1 < 25$ km. Jordan et al. (1983) calculated a similar mean ξ of 0.213 ± 0.011 from multibeam and wide-beam surveys of eastern Pacific seamounts. For 35 large western Pacific seamounts with $a_1 > 25$ km, $h = 0.007a_1 + 4254 \pm 488$ m. The decrease in h/a_1 for large seamounts does not reflect a decrease in slope but rather the predominance of flat-topped guyots and atolls. The average slope $\theta = 11 \pm 3°$ is independent of seamount size. There is considerable scatter in the flatnesses $f = a_2/a_1$ for the guyots and atolls. The 42-point sample has a mean of 0.40 ± 0.177.

Seafloor depth was assumed to be 6 km for the modeled seamounts. The edifices were given densities of 2.6 g/cm^3 and gravity anomalies were calculated for all five "uncompensated" models (Figure 8). The excess mass of the five model edifices was then assumed to be completely isostatically compensated by thickening of the crust (2.9 g/cm^3) beneath them, i.e. Airy isostasy, and gravity anomalies were calculated (Figure 8). Note that the model for the completely locally compensated atoll predicts that the crust mantle boundary lies at a depth of 31 km beneath the atoll. The calculated gravity field for the largest compensated model has negative anomalies flanking the edifice and the maximum amplitude (170 mgal) is 200 mgal lower than that calculated for the uncompensated model (370 mgal). This is approximately the range of gravity anomalies observed on western Pacific islands. In Figure 11 the maximum calculated gravity anomalies are plotted as a function of minimum depth to the tops of the models. As the depths to the seamounts increase, the predicted values converge.

We have also modeled seamounts using exact expressions for the on-axis vertical component of the gravity anomaly for a cone or a frustrum of a cone. This problem is one that has been considered before although this derivation was done independently. Previous efforts in this area include the derivation of the anomaly at points off-axis for a circular disk or vertical cylinder (Parasnis, 1961), for a right circular cone (Schwank and Lazarewicz, 1982), and the work of Moon (1981) and Jenkins et al. (1983) which have focused on deriving analytical expressions for more complex cases where the density is laterally varying. Our derivation assumes constant density for the structure, although more complex density distributions may be constructed by superposition.

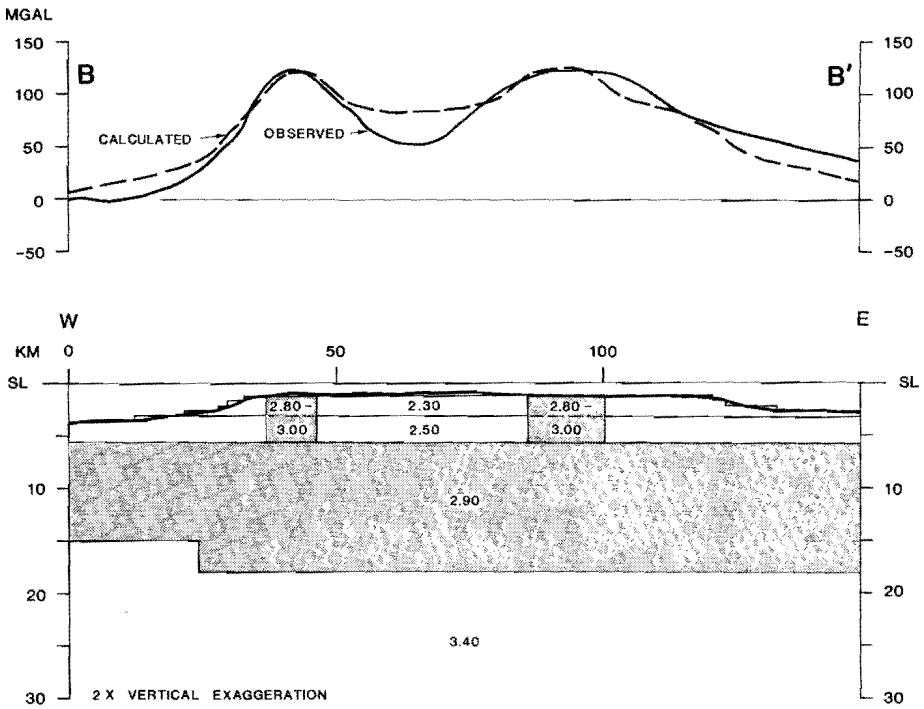

Fig. 6. Cross-section of the density model for Ita Mai Tai Guyot showing observed (solid line) and calculated (dashed line) gravity anomalies (Wedgeworth, 1985; Wedgeworth and Kellogg, this volume). Location shown in Figure 4.

We calculate the anomaly by stacking thin disks of varying radii atop each other and summing the anomaly due to each disk. If the radius of each disk varies linearly with the depth, then the structure obtained is either a cone or a frustrum of a cone. All disks are assumed to have the same density ρ. In the limit that the thickness of each disk becomes infinitesimal, the sum becomes an integral. The on-axis vertical gravitational attraction dg_z of a thin horizontal circular disk of thickness dz and radius a is

$$dg_z = 2\pi G(\rho - \rho_w)dz(1 - z/\sqrt{z^2 + a^2}) \quad (1)$$

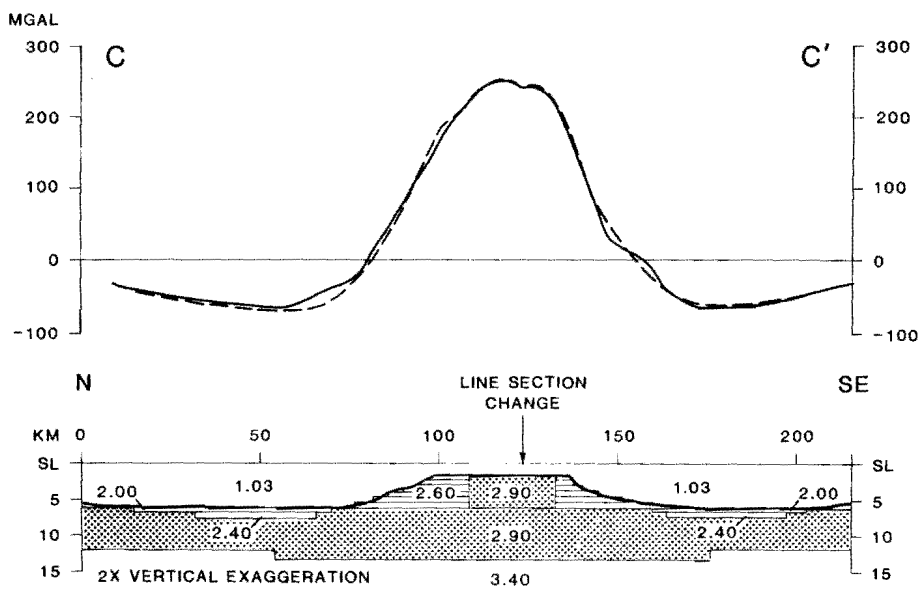

Fig. 7. Cross-section of Sio Guyot with two dense vertical prisms (Kellogg and Ogujiofor, 1985). Location shown in Figure 3.

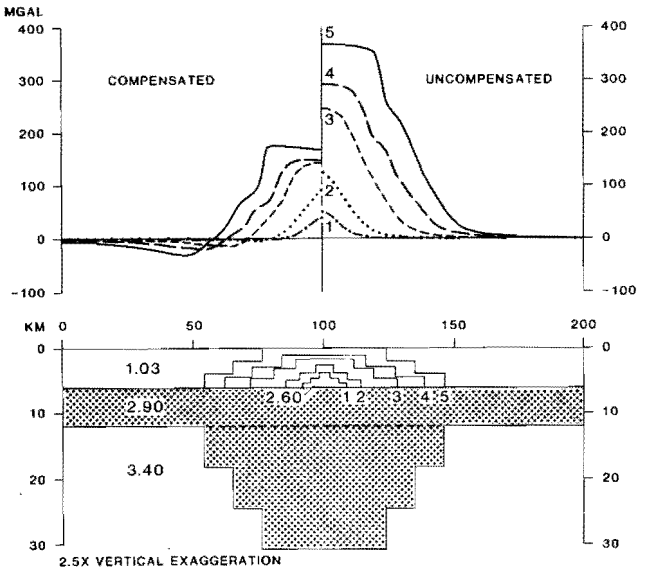

Fig. 8. Cross-sections of polygonal prism models. The calculated gravity is for isostatically compensated seamounts ($\mu = 100\%$) on the left and uncompensated seamounts ($\mu = 0$) on the right. A thickened crustal root is shown for a completely locally compensated atoll.

where G is the gravitational constant, ρ_w is the density of water and z is the depth (e.g. Rose and Bowman, 1974). If $a(z) = bz + c$ in the interval $[z_0, z_1]$, then

$$g_z(z_0, z_1) = \int_{z_0}^{z_1} dg_z \qquad (2)$$
$$= \int_{z_0}^{z_1} 2\pi G(\rho - \rho_w)\left[1 - \frac{z}{\sqrt{z^2 + (bz + c)^2}}\right] dz$$

The evaluation of this integral is straightforward. Writing

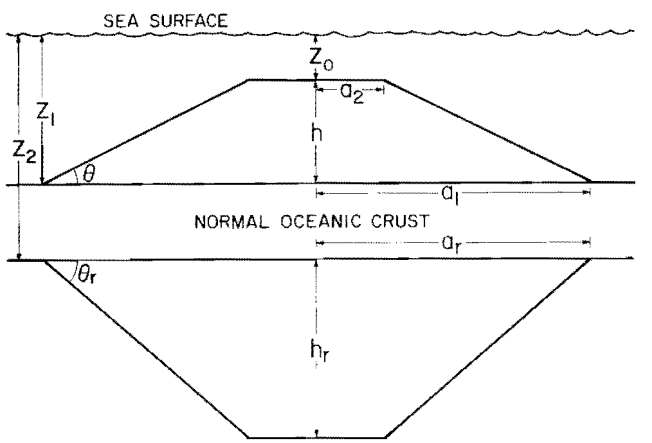

Fig. 9. Cross-section of a flat-topped seamount and thickened crustal root with cylindrical symmetry. Adopting the terminology of Jordan et al. (1983), its shape is described by the flatness $f = a_2/a_1$ and the height-to-radius ratio $\xi = h/a_1$.

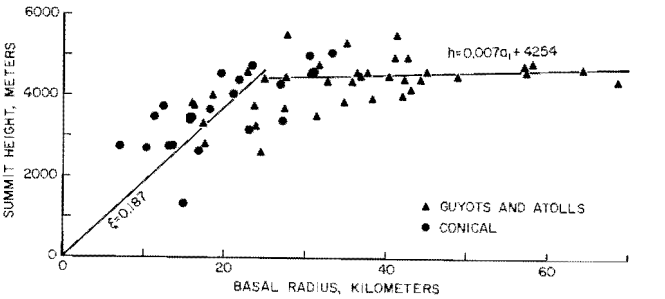

Fig. 10. Summit height h versus basal radius a_1 for 63 seamounts and islands in the western Pacific. For 28 small seamounts ($a_1 < 25$ km), the mean height-to-basal radius ration $\xi = 0.187 \pm 0.056$. For 35 large seamounts ($a_1 > 25$ km), $h = 0.007a_1 + 4254 \pm 488$ m.

$$I(z, b, c) = 2\pi G(\rho - \rho_w)\left[z - \frac{1}{\beta}\sqrt{z^2 + 2bcz/\beta^2 + c^2/\beta^2}\right.$$
$$\left. + \frac{bc}{\beta^3}\ln\left(z + \frac{bc}{\beta^2} + \sqrt{z^2 + 2bcz/\beta^2 + c^2/\beta^2}\right)\right] \qquad (3)$$

where $\beta^2 = 1 + b^2$, then

$$g_z(z_0, z_1) = I(z_1, b, c) - I(z_0, b, c) \qquad (4)$$

If the slope of the seamount is θ, then $b = \cot\theta$ and $\beta = 1/\sin\theta$. If the radius a at some depth is known, then c can be determined: $c = a(z) - bz$. The calculated gravity-depth functions are plotted in Figure 11 for uncompensated conical seamounts of density 2.6 g/cm^3, slope = 10°, and seafloor depth = 6 km. Values are also shown for Airy compensated seamounts where the excess mass of the seamount edifice is locally compensated by a low density crustal root beneath the seamount (Figure 9). The gravity effect of the root is

$$g_r(z_2, z_2 + h_r) = I(z_2 + h_r, b_r, c_r) - I(z_2, b_r, c_r) \qquad (5)$$

where $z_2 - z_1$ = normal oceanic crustal thickness = 6 km, h_r = thickness of root, $a_r(z) = b_r z + c_r$ gives the radius of the root and $\Delta\rho = \rho_r - \rho_m = -0.5$ g/cm^3. Gravity values are also plotted for shallow (0-2km), flat-topped seamounts (guyots and atolls) with constant flatness ratios $f = a_2/a_1 = 0.37$ (Figure 9).

Figure 12 illustrates the seafloor depth dependence of the on-axis gravity anomalies. Sea surface gravity anomalies are calculated for uncompensated conical seamounts of density 2.3 g/cm^3 , slope = 10° for seafloor depths of 1 to 6 km.

Free-air gravity-depth curves calculated from Equations (4) and (5) are superimposed on the observed data for 97 western Pacific seamounts in Figure 13. The curves were calculated for shallow (0-1.75 km) flat-topped seamounts, $f = 0.37$, and deeper (1.5-4.0 km) conical seamounts, $\theta = 10°$, $\rho = 2.6$ g/cm^3. The uncompensated curves shown are for a seafloor depth of 6 km; the compensated curves shown are for a seafloor depth of 4.5 km. The observed data for all 38 islands and atolls and for 55 of the 59 seamounts lies within the range of predicted values. In other words, about 96% of the wide variations in observed gravity signatures for western Pacific seamounts can be explained by different levels of Airy isostatic compensation. The three seamounts to the right of the predicted field (Suiko, Nintoku, and Unnamed) are all part of the Emperor chain and appear to have anomalously high mean densities (2.7 - 2.9 g/cm^3). The seamount to the left of the field (Chatauqua) is located on the Hawaiian arch.

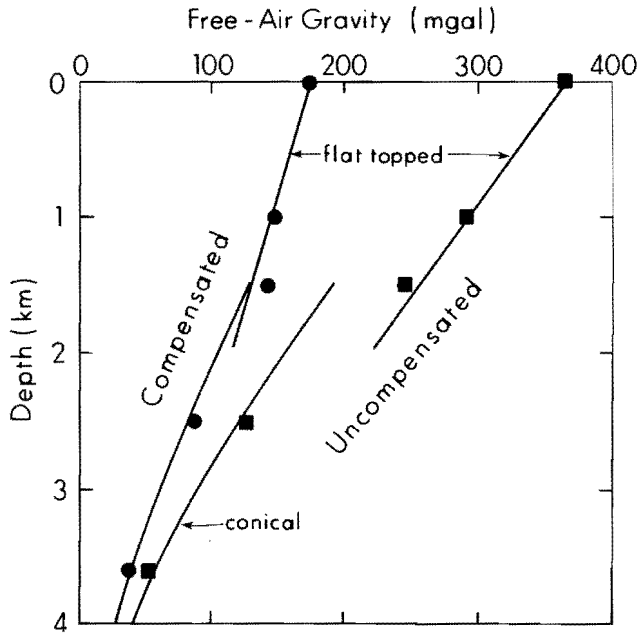

Fig. 11. Maximum calculated gravity anomalies versus minimum depth to seamount models. The squares and circles are for uncompensated ($\mu = 0$) and compensated ($\mu = 100\%$) polygonal prism models respectively (Figure 8). The solid lines are calculated from Equations (4) and (5) for deep conical seamounts ($\theta = 10°$, $z_1 = 6$ km, $z_2 = 12$ km) and shallow flat-topped seamounts ($f = 0.37$).

The abrupt increase in maximum gravity anomalies observed over seamounts shallower than 1.7 km (Figure 13) corresponds approximately to the depth range of guyots in the western Pacific.

Lithospheric Flexure and Crustal Intrusion

Isostatic compensation for seamounts and islands is probably achieved by lithospheric flexure and phase changes or sill intrusions in the lower crust. The gravity signatures that would be produced by lithospheric flexure or crustal intrusion are indistinguishable, so seismic data must be used to determine the compensation mechanism. Many investigations (See for example, Walcott, 1970; Watts et al., 1975) have been undertaken to study the deformation of the oceanic lithosphere by the weight of seamounts. The response of the oceanic lithosphere to long-term surface loads is modeled as that of an elastic plate overlying a weak fluid. Flexure of the lithosphere can explain much of the gravity signature of seamounts. However, a two-ship multichannel seismic experiment around Oahu (Watts et al., 1985) showed that much of the crustal thickening could not be explained by the simple flexural model. The wide-angle seismic profiles obtained by HIG and Lamont-Doherty Geological Observatory in August and September of 1982 show the M-discontinuity dipping 8 km to a depth of 19 km under the Hawaiian Ridge. Reflectors near the top of the crust, however, dip only 2 or 3 km to a depth of 7 or 8 km under the ridge. The remaining 5 or 6 km of crustal thickness may be tholeiitic (Watts et al., 1985) and plagioclase- bearing pyroxene (Sen, 1983) magma intruded into the crust under Oahu.

Isostatic Compensation and Age of Loading

As the oceanic lithosphere moves away from the ridge crest, it cools and thickens so that its effective elastic thickness is increased. Watts and Ribe (1984) noted that seamounts formed on young seafloor near ridge crests are often associated with short wavelength, low amplitude gravity anomalies, and thin effective elastic lithosphere thicknesses. It follows that seamounts formed on young seafloor near ridge crests should also be in local isostatic equilibrium.

We define the degree of local compensation μ as the ratio of the mass deficiency below the normal crust to the excess mass above the normal crust. Since the volume of a right circular cone is proportional to its height, it follows that the thickness of the low-density crustal root h_r (Figure 9) will be proportional to μ, $h_r = \mu h_{Airy}$, where h_{Airy} is the root thickness for a 100% compensated seamount. The free-air gravity anomaly due to the seamount plus the root is

$$g_{observed} = g_z(z_0, z_1) + g_r(z_2, z_2 + \mu h_{Airy}) \tag{6}$$

Equation (6) can be inverted by an iterative process to determine the degree of compensation μ from the free air anomaly and the shape and depth of the seamount. The expression for g_r includes a term linear in μ and two terms non-linear in μ. We take the first approximation by ignoring the non-linear terms,

$$\mu_{(1)} = \frac{g_{observed} - g_z(z_0, z_1)}{2\pi G(\rho_m - \rho_c)h_{Airy}} \tag{7}$$

where ρ_c is the density of the crustal root and ρ_m is the mantle density. We can then solve for μ by an iterative process using the equation

$$\mu_{(n+1)} = \mu_{(1)} + \frac{1}{\mu_{(n)}h_{Airy}}\left[\frac{1}{\beta_r}\sqrt{z^2 + 2b_r c_r z/\beta_r^2 + c_r^2/\beta_r^2} + \frac{b_r c_r}{\beta_r^3}\ln\left(z + \frac{b_r c_r}{\beta_r^2} + \sqrt{z^2 + 2b_r c_r z/\beta_r^2 + c_r^2/\beta_r^2}\right)\right]_{z_2}^{z_2+\mu_n h_{Airy}} \tag{8}$$

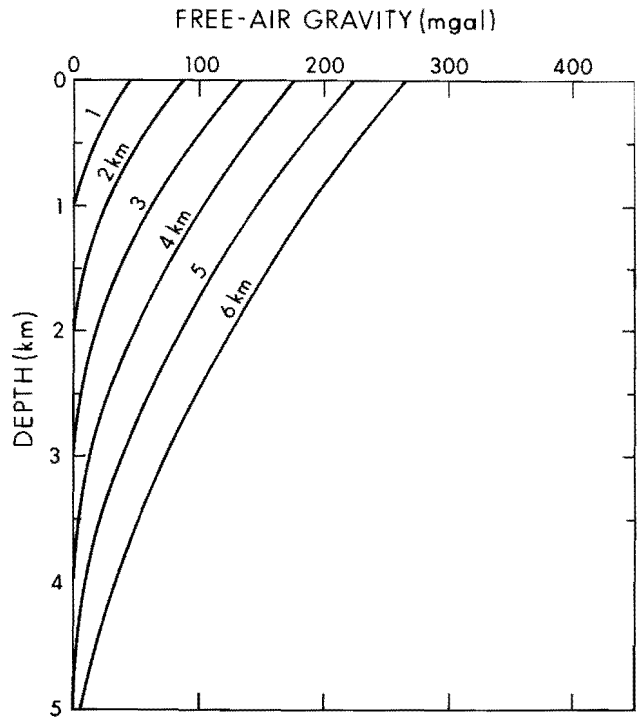

Fig. 12. On-axis gravity versus depth to seamount top for uncompensated conical seamounts of density 2.3 g/cm^3, slope = 10°, and seafloor depths of 1 to 6 km.

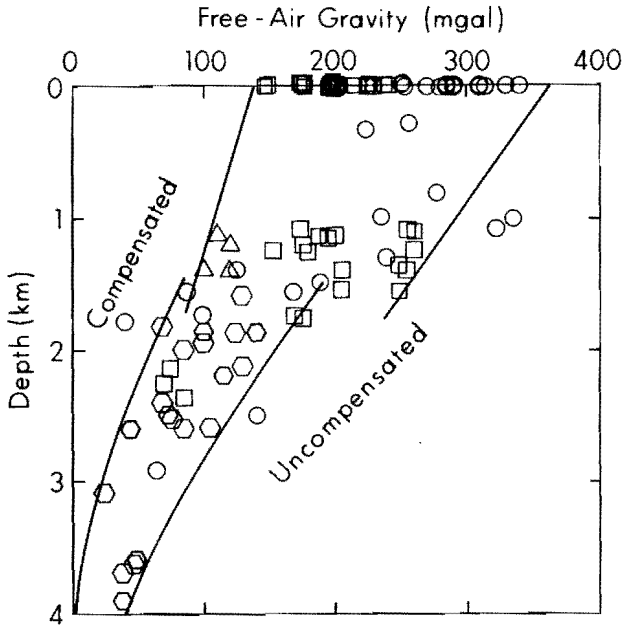

Fig. 13. Free-air gravity/depth curves calculated from Equations (4) and (5) superimposed on the observed data from Figure 1. The curves are calculated for shallow flat-topped seamounts, $f = 0.37$, and deeper conical seamounts, $\theta = 10°$, $\rho = 2.6 g/cm^3$. For uncompensated ($\mu = 0$) curves $z_1 = 6$ km; for compensated ($\mu = 100\%$) curves, $z_1 = 4.5$ km. About 96% of the observed data lies within this range of calculated values.

The algorithm converges more slowly for small structures because there is a smaller difference between the gravity signatures of small uncompensated seamounts and small compensated seamounts than for the corresponding difference for larger seamounts.

Table 1 shows estimates of μ and the age of the oceanic lithosphere at the time of loading t for five well-dated islands and one seamount. The estimated errors in μ are based on the following uncertainties: maximum FAA $\pm$ 10 mgal, $z_0 \pm$ 150 m, $z_1 \pm$ 300 m, $a_1 \pm$ 20%, and $a_2 \pm$ 20%. The uncertainty in the compensation estimate increases with increasing depth z_0, increasing μ, and with decreasing a_1, a_2, and $z_1 - z_0$.

Volcanic edifices erupted on young seafloor, such as Iceland or Galapagos (Isabela Island) are much closer to local isostatic equilibrium than edifices formed on old lithosphere, such as Hawaii and Pohnpei (Figure 14). The curve shown in Figure 14 is a least squares fit to the μ and $t^{1/2}$ values,

$$\mu(\%) = 68 - 5.6t^{1/2} \quad (9)$$

The standard deviation is $\pm$ 0.8 for the slope and $\pm$ 6.5 for the intercept. The curve is similar in shape to oceanic isotherms based on the cooling plate model (Parsons and Sclater, 1977) and elastic thickness of the lithosphere at the time of loading (Watts and Ribe, 1984). The similarity in shape suggests that the results of the isostatic compensation algorithm used in this study are quantitatively consistent with the predictions of the lithospheric flexure method and that some of the isostatic compensation is caused by flexure of the lithosphere. Several advantages of the method used here are that it does not rely on a particular mechanical model and it can be rapidly applied to large data sets (Kellogg and Freymueller, 1986).

Potassium-argon ages for 16 rock samples from Kusaie and Pohnpei range from 1.2 $\pm$ 0.1 to 8.6 $\pm$ 0.6 m.y. (Keating et al., 1984). Epp (1984) estimates the ages of loading t as approximately 152 and 160 m.y. respectively for Kusaie and Pohnpei. If correct, these ages double the duration of the window of vulnerability of the lithosphere to seamount formation proposed by Watts and Ribe (1984).

The results in Figure 14 have important implications for studies of the geological evolution of seamounts, oceanic islands, and the ocean basins. By determining the relative isostatic compensation level of a volcanic edifice, it should be possible to estimate the age of the seafloor t at the time the edifice was emplaced. Because of the slope of the curve in Figure 14, these estimates should be most reliable for $t < 30$ m.y. For example, Sio Guyot in the Mid-Pacific Mountains has a maximum FAA of 120 mgal, a minimum depth of 1130 m and average seafloor depth of 5550 m. Using Equation (8), $\mu = 71\% \pm 15\%$, and $h_r = 9.9$ km. The maximum calculated depth to the crust-mantle boundary is 21.5 km. This depth estimate compares well with the 22 $\pm$ 2 km estimate derived from detailed 3-dimensional modeling of Sio Guyot (Kellogg and Ogujiofor, 1985). From Equation (8) the age of loading t is 0-5 m.y., i.e. a ridge-crest origin. Tholeiites of the Mid-Pacific Mountains resemble lavas of Iceland and the Galapagos Islands. Kroenke et al. (1985) interpreted the orthogonal fault system, low gravity anomalies, and lava chemistry of the Mid-Pacific Mountains as the result of plateau eruption along an Early Cretaceous rift system followed by the formation of the upper edifices, including those of Sio Guyot 10 to 20 m.y. later.

Regional Clustering of Compensation Levels

Although variations in isostatic compensation levels can explain the observed range of gravity and geoid anomalies associated with

TABLE 1. Age of Loading and Parameters for Calculating Seamount Compensation

Seamount or Island	Observed Gravity g_{obs} (mgal)	Seafloor Depth z_1 (km)	f	ξ	Compensation μ (%)*	Age of Edifice t_e (myBP)	Age of Lithosphere t_l (myBP)	Age of Lithosphere at Time of Loading $t = t_l - t_e$ (my)**
Iceland	60	2.5	0.56	0.01	65 $\pm$ 10	0.0	5	5 $\pm$ 5
Galapagos***	120	3.0	0.63	0.03	44 $\pm$ 11	0.0	10	10 $\pm$ 2
Tahiti	230	4.4	0.33	0.07	23 $\pm$ 13	1.0	66	65 $\pm$ 5
Great Meteor	250	4.8	0.40	0.08	15 $\pm$ 17	11.0	84	73 $\pm$ 2
Hawaii	307	5.4	0.55	0.05	13 $\pm$ 09	0.0	92	92 $\pm$ 5
Pohnpei	290	4.75	0.27	0.07	3 $\pm$ 14	5.4	165	160 $\pm$ 10

*Computed assuming $z_o = 0$ (except Great Meteor 0.25), $z_2 = z_1 + 6$ km, $\rho_w = 1.03$ g/cm^3,
$\rho = 2.6$ g/cm^3, $\rho_c = 2.9$ g/cm^3, and $\rho_m = 3.4$ g/cm^3 from Equation (10).
$f = a_2/a_1$ (Figure 9). $\xi = h/a_1$ (Figure 10).
**Reference for ages: Epp (1984) except Great Meteor from Verhoef (1984).
***Parameters for Isabela Island.

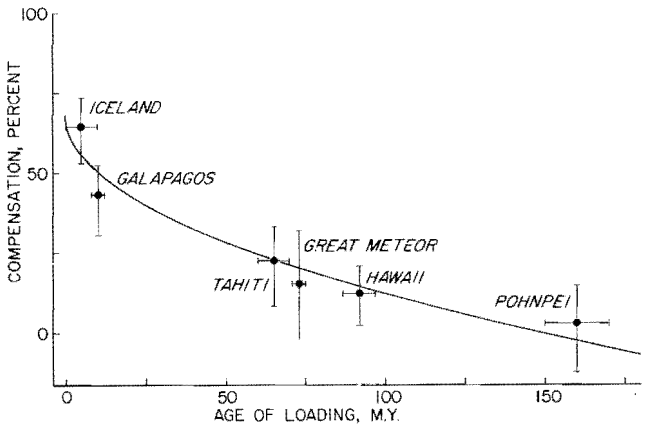

Fig. 14. Plot of degree of isostatic compensation μ against age of the lithosphere at the time of loading t from Table 1. The curve shown is $\mu(\%) = 68 - 5.6t^{1/2}$.

seamounts and islands, it would be impossible to predict bathymetry directly from satellite altimetry unless compensation levels are consistent and known for a region of the ocean.

In Figure 15 depth-corrected free-air gravity anomalies are contoured for seamounts in the western Pacific to see if there are systematic spatial variations in the seamount gravity-depth relationship. The gravity values were corrected for depth by subtracting $(3800 - z_0)/16$ from the observed maximum anomalies.

Seamounts in the East Mariana Basin have positive gravity anomalies, over 100 mgal, in sharp contrast to the negative anomalies, as low as -78 mgal, in the Marshall Island Group and in the Mid-Pacific Mountains. As discussed in this paper, detailed three-dimensional forward modeling of the gravity field for Sio Guyot in the Mid-Pacific Mountains shows that the negative residual may be accounted for by isostatic compensation. Inversion of the gravity field for Ita Mai Tai Guyot indicates that the positive residual may be explained by a lack of compensation. Such systematic spatial variations in compensation levels may be used to infer the tectonic origins (ridge crest versus mid-plate) and ages of seamount clusters.

Discussion

Detailed modeling of two large seamounts in the western Pacific, Sio and Ita Mai Tai Guyots, shows that the large contrast in their sea surface gravity fields is probably not a function of density differences in the two seamounts but rather a function of different depths to the crust-mantle boundary. The depths to the Moho are proportional to the Airy isostatic compensation levels for seamounts and, as predicted by elastic cooling plate models, are inversely proportional to the root of the seafloor age at the time of loading. However, a two-ship multichannel seismic experiment around Oahu (Watts et al., 1985) showed that much of the crustal thickening may not be explained by the simple flexural model. The crust may be thickened by the intrusion of large volumes of tholeiitic (Watts et al., 1985) and plagioclase-bearing

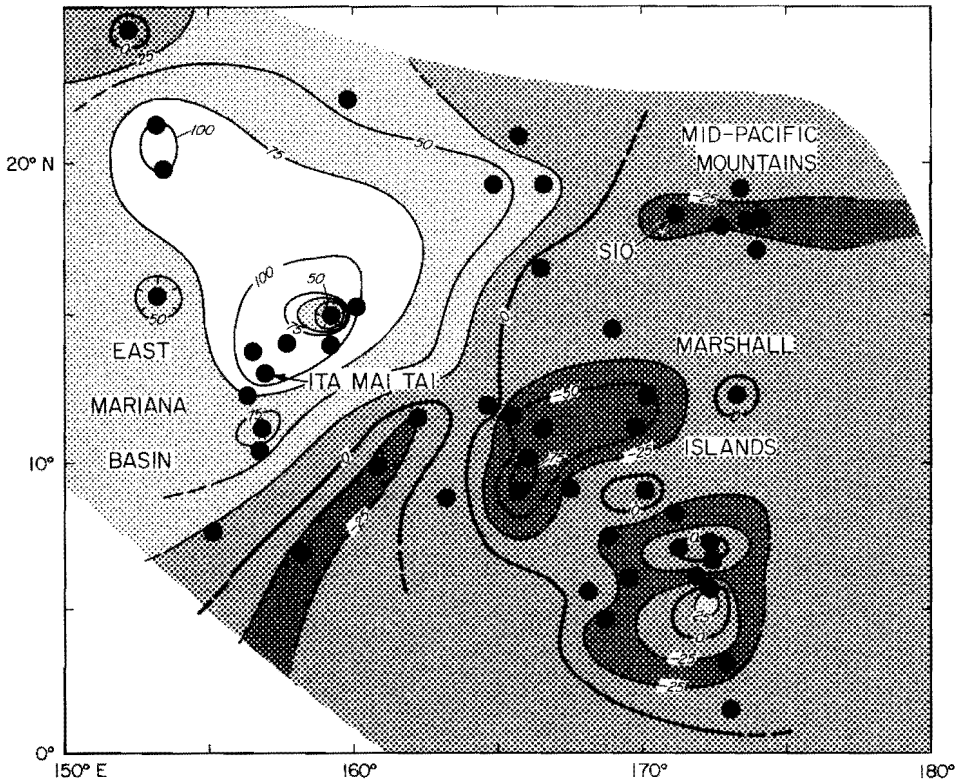

Fig. 15. Depth-corrected on-axis free-air gravity anomalies for seamounts in the western Pacific. The on-axis gravity values were corrected for depth by subtracting $(3800 - z_o)/16$ from the observed maximum anomalies. The discrete point gravity values were contoured to facilitate pattern recognition. Note the clustering of seamounts with positive gravity residuals in the East Mariana Basin.

pyroxene magma (Sen, 1983). Bending and thickening of the crust can explain the anomalously low gravity fields observed over many seamounts and islands that were previously interpreted as caused by magma chambers or thermal anomalies (e.g., Le Pichon and Talwani, 1964; Case et al., 1973).

It is impossible to completely explain the variability in seamount gravity signatures by different edifice densities. In fact, direct measurements of seamount and oceanic island rock densities, seismic compressional velocities, and inversion of the gravity fields over uncompensated seamounts suggest a mean density of 2.6 g/cm^3 with an uncertainty of only about $\pm$ 0.2 g/cm^3. From the gravity fields and bathymetry, Ishihara (this volume) determined the mean density of 19 seamounts in the Bonin Arc to be 2.66 $\pm$ 0.13 g/cm^3. These mean values are lower than the 2.8 g/cm^3 value common in the geophysical literature. Of the 97 seamounts included in this study, only three seamounts in the Emperor chain have anomalously high mean densities (2.7 - 2.9 g/cm^3).

Precise models of Ita Mai Tai (Figures 4 and 6) and Sio Guyots (Figures 3 and 7) and Oahu and Hawaii Islands show that dense conduits contribute substantially to the small wavelength observed sea surface gravity fields. The conduits are fracture zones 5 to 17 km in diameter containing dunites, spinel pyroxenites, nepheline monzonites, theralites, and essexites extending into the lower crust.

A simple method has been presented in this paper for the rapid estimation of seamount isostatic compensation levels. Seamounts are approximated as cones or frustrums of cones, and the observed on-axis vertical gravitational attraction is inverted by an iterative process (Equation 8) to determine the degree of Airy compensation. The algorithm is independent of mechanical assumptions regarding oceanic lithosphere, involves low computational costs, and is particularly useful for the rapid evaluation of large data sets. The results and associated uncertainties are comparable to those of detailed 3-dimensional models and frequency domain studies. The generalized forward problem can also be addressed using exact expressions for the on-axis vertical component of gravity for a cone or a frustrum of a cone. The predicted anomalies for compensated and uncompensated seamounts (Figure 11) converge rapidly at depths of 2 km or greater, making the inversion of the gravity values to estimate compensation levels or flexural parameters much more difficult for small deep edifices such as the Musicians Seamounts (Schwank and Lazarewicz, 1982; Dixon et al., 1983; Freedman and Parsons, 1986).

Because of the wide variation in observed geoid signatures of seamounts, a successful short-wavelength bathymetric transfer function for satellite altimeter data must be based on a statistically representative sample. The data presented in this paper shows the range of gravity/depth values for 97 well-surveyed seamounts in the western Pacific. A depth-corrected maximum free-air gravity anomaly map for seamounts in the western Pacific (Figure 15) suggests regional variations in isostatic compensation levels. Observed gravity and bathymetry can be readily inverted using the algorithm presented in this paper to estimate the compensation levels of well-surveyed seamounts. If the systematic spatial variations observed in the western Pacific are representative, then we can infer the tectonic origin of seamounts elsewhere and develop regional bathymetric-satellite altimetry transfer functions.

Acknowledgments. The first author is thankful to H. William Menard for introducing him to enigmas concerning Pacific seamount morphology in a seminar eleven years ago. We thank L.W. Kroenke and the scientists and crew of the R/V KANA KEOKI for their help in the collection of data from the Mid-Pacific Mountains and for introducing the first author to geophysics at sea. J.F. Campbell kindly provided unpublished gravity data for seamounts in the East Mariana Basin and the Marshall Island Group. J. Rose suggested generalizing seamount gravity models with exact expressions for gravity over right circular cones and frustrums of cones. W. Strange and G. Sen convinced us of the importance of dense conduit zones in the structures of seamounts and volcanic islands. The manuscript was improved with the helpful reviews of A. Lazarewicz and L. Dorman. S. Dang drafted most of the figures, K. Chainey and C. Yasui helped with the typing, and D. Henderson proofread the manuscript. This research was supported by the Office of Naval Research, Code 425GG. Hawaii Institute of Geophysics contribution no. 1866.

References

Case, J.E., S.L. Ryland, T. Simkin, and K.A. Howard, Gravitational evidence for a low-density mass beneath the Galapagos Islands, *Science, 181*, 1040-1042, 1973.

Dixon, T.H., M. Naraghi, M.K. McNutt, and S.M. Smith, Bathymetric prediction from SEASAT altimeter data, *J. Geophys. Res., 88*, 1563-1571, 1983.

Eaton, J.P., Crustal structure and volcanism in Hawaii, in *The Crust of the Pacific Basin, Geophys. Monogr. Ser.*, vol. 6, edited by G.A. Macdonald and H. Kuno, pp. 13-29, AGU, Washington, D.C., 1962.

Epp, D., Implications of volcano and swell heights for thinning of the lithosphere by hotspots, *J. Geophys. Res., 89*, 9991-9996, 1984.

Furumoto, A.S., and G.P. Woollard, Seismic refraction studies of the crustal structure of the Hawaiian Archipelago, *Pacific Science, 19*, 315-319, 1965.

Furumoto, A.S., N.J. Thompson, and G.P. Woollard, The structure of Koolau Volcano from seismic refraction studies, *Pacific Science, 19*, 306-314, 1965.

Furumoto, A.S., G.P. Woollard, J.F. Campbell, and D.M. Hussong, Variation in the thickness of the crust in the Hawaiian Archipelago, in *The Crust and Upper Mantle of the Pacific Area, Geophys. Monogr. Ser.*, vol. 12, edited by L. Knopoff, C.L. Drake, and P.J. Hart, pp. 94-111, AGU, Washington, D.C., 1968.

Freedman, A.P., and B. Parsons, Seasat-derived gravity over the Musicians Seamounts, *J. Geophys. Res., 91*, 8325-8340, 1986.

Harrison, J.C., and W.C. Brisbin, Gravity anomalies off the west coast of North America. 1: Seamount Jasper, *Geol. Soc. Amer. Bull., 70*, 929-934, 1959.

Hill, D.P., and J.J. Zucca, Constraints on the structure of Kilauea and Mauna Loa Volcanoes, Hawaii, and some implications for seismomagmatic processes, in *Transactions of Conference on how volcanoes work*, Hilo, Hawaii, 1987.

Ishihara, T., Gravimetric determination of densities of seamounts along the Bonin Arc, this volume.

Jenkins, A.J.O., D. Messfin, and W. Moon, Gravity modelling of salt domes and pinnacle reefs, *J. Canadian Soc. Expl. Geophys., 19*, 51-56, 1983.

Jordan, T.H., H.W. Menard, and D.K. Smith, Density and size distribution of seamounts in the eastern Pacific inferred from wide-beam sounding data, *J. Geophys. Res., 88*, 10508-10518, 1983.

Keating, B.H., D.P. Mattey, C.E. Helsley, J.J. Naughton, D. Epp, A. Lazarewicz, and D. Schwank, Evidence for a hot spot origin of the Caroline Islands, *J. Geophys. Res., 89*, 9937-9948, 1984.

Kellogg, J.N., and I.J. Ogujiofor, Gravity field analysis of Sio Guyot: An isostatically compensated seamount in the Mid-Pacific Mountains, *Geo- Marine Letters, 5*, 91-97, 1985.

Kellogg, J.N., and J.T. Freymueller, Isostatic compensation of western Pacific seamounts (abstract), *Eos Trans. AGU, 67*, 1229, 1986.

Kinoshita, W.T., H.L. Krivoy, D.R. Mabey, and R.R. MacDonald, Gravity survey of the Island of Hawaii, *U.S. Geol. Surv. Prof. Pap., 475-C*, 114-116, 1963.

Kroenke, L.W., D.A. Walker, and G.L. Maynard, Gravity measurements of Midway Island and reef (abstract), *Proceedings of the Eleventh Pacific Science Congress*, Tokyo, 1966.

Kroenke, L.W., J.N. Kellogg, and K. Nemoto, Mid-Pacific Mountains revisited, *Geo-Marine Letters, 5*, 77-81, 1985.

Laughton, A.S., M.N. Hill, and T.D. Allan, Geophysical investigations of a seamount 150 miles north of Madeira, *Deep-Sea Research, 7*, 117-141, 1960.

Lazarewicz, A.R., and D.C. Schwank, Locating uncharted seamounts using satellite altimetry, *Geophys. Res. Lett., 9*, 385-388, 1982.

Lewis, B.T.R., and L.R. Dorman, Experimental Isostasy II: An isostatic model for the U.S.A. derived from gravity and topographic data, *J. Geophys. Res., 75*, 3367-3386, 1970.

LePichon, X., and M. Talwani, Gravity survey of a seamount near 35°N 46°W in the North Atlantic, *Marine Geology, 2*, 262-277, 1964.

Machesky, L.F., Gravity relations in American Samoa and the Society Islands, *Pacific Science, 19*, 367-373, 1965.

Manghnani, M.H., and G.P. Woollard, Ultrasonic velocities and related elastic properties of Hawaiian basaltic rocks, *Pacific Science, 19*, 291-295, 1965.

Moon, W., A new method of computing geopotential fields, *Geophys. J. Roy. Astron. Soc., 67*, 735-746, 1981.

Nafe, J.E., and C.L. Drake, Physical properties of marine sediments, in *The Sea*, vol. 3, edited by M.N. Hill, pp. 85-102, John Wiley and Sons, New York, 1963.

Nayudu, Y.R., A new hypothesis for the origin of guyot and seamount terraces, in *The Crust of the Pacific Basin, Geophys. Monogr. Ser.*, vol. 6, edited by G.A. Macdonald and H. Kuno, pp. 171-180, AGU, Washington, D.C., 1962.

Nemoto, K., and L.W. Kroenke, Sio Guyot: a complex volcanic edifice in the western Mid-Pacific Mountains, *Geo-Marine Letters, 5*, 83-89, 1985.

Nettleton, L.L., Determination of density for reduction of gravimeter observations, *Geophysics, 4*, 176-183, 1939.

Officer, C.G., M. Ewing, and P.C. Wuenschel, Seismic refraction measurements in the Atlantic Ocean Basin. 4: Bermuda, Bermuda Rise, and Nares Basin, *Geol. Soc. Amer. Bull., 63*, 777-808, 1952.

Parasnis, D.S., Exact expressions for the gravitational attraction of a circular lamina at all points of space and of a right circular vertical cylinder at points external to it, *Geophysical Prospecting, 9*, 382, 1961.

Parsons, B., and J.G. Sclater, An analysis of the variation of ocean floor bathymetry and heat flow with age, *J. Geophys. Res., 82*, 803-828, 1977.

Plouff, D., Gravity and magnetic fields of polygonal prisms and application to magnetic terrain corrections, *Geophysics, 41*, 727-741, 1976.

Raitt, R.W., Bikini and nearby atolls. 3: Geophysics, Seismic refraction studies of Bikini and Kwajalein Atolls and Sylvania Guyot, *U.S. Geol. Surv. Prof. Pap., 260K*, pp. 507-524, 1954.

Robertson, E.I., Gravity survey in the Cook Islands, *N.Z. J. Geol. Geophys., 10*, 1484-1498, 1967.

Robertson, E.I., Additional gravity surveys in the Cook Islands, *N.Z. J. Geol. Geophys., 13*, 184-198, 1970.

Roedder, E., Liquid CO_2 inclusions in olivine-bearing nodules and phenocrysts from basalts, *Am. Mineral., 50*, 1740-1782, 1965.

Rose, J.C., and B.R. Bowman, The effect of seamounts and other bottom topography on marine gravity anomalies, in *Proceedings of the International Symposium on Applications of Marine Geodesy, Marine Technology Society*, 381- 396, 1974.

Ryan, M.P., R.Y. Kyonanagi, and R.S. Fiske, Modeling the three-dimensional structure of macroscopic magma transport systems: application to Kilauea volcano, Hawaii, *J. Geophys. Res., 86*, 7111-7129, 1981.

Sager, W.W., G.T. Davis, B.H. Keating, and J.A. Philpotts, A geophysical and geologic study of Nagata Seamount, northern Line Islands, *Journal Geomagnetism and Geoelectricity, 34*, 283-305, 1982.

Schwank, D.C., and A.R. Lazarewicz, Estimation of seamount compensation using satellite altimetry, *Geophys. Res. Lett., 9*, 907-910, 1982.

Scientific Party, Leg 89, Leg 89 drills Cretaceous volcanics, *Geotimes, 28*, 17-20, 1983.

Sen, G., A petrologic model for the constitution of the upper mantle and crust of the Koolau shield, Oahu, Hawaii, and Hawaiian magmatism, *Earth Planet. Sci. Lett., 62*, 215-228, 1983.

Shor, G.G., and D.D. Pollard, Mohole site selection studies north of Maui, *J. Geophys. Res., 69*, 1627-1637, 1964.

Strange, W.E., G.P. Woollard, and J.C. Rose, An analysis of the gravity field over the Hawaiian Islands in terms of crustal structure, *Pacific Science, 19*, 381-389, 1965.

Suyenaga, W., Isostasy and flexure of the lithosphere under the Hawaiian Islands, *J. Geophys. Res., 84*, 5599-5604, 1979.

Swanson, D.A., W.A. Duffield, and R.S. Fiske, Displacement of the south flank of the Kilauea volcano: the result of forceful intrusion of magma into the rift zones, *U.S. Geol. Surv. Prof. Pap., 963*, 39 p., 1976.

Talandier, J., and E.A. Okal, Crustal structure in the Society and Tuamotu Islands, French Polynesia, *Geophys. J. Roy. Astron. Soc.*, in press.

Vogt, P.R., B. Zondek, P.W. Fell, N.Z. Cherkis, and R.K. Perry, Seasat altimetry, the North Atlantic geoid, and evaluation by shipborne subsatellite profiles, *J. Geophys. Res., 89*, 9885-9903, 1984.

Walcott, R.I., Flexural rigidity, thickness, and viscosity of the lithosphere, *J. Geophys. Res., 75*, 3941-3954, 1970.

Watts, A.B., and N.M. Ribe, On geoid heights and flexure of the lithosphere at seamounts, *J. Geophys. Res., 89*, 11152-11170, 1984.

Watts, A.B., J.R. Cochran, and G. Selzer, Gravity anomalies and flexure of the lithosphere: a three-dimensional study of the Great Meteor Seamount, Northeast Atlantic, *J. Geophys. Res., 80*, 1391-1398, 1975.

Watts, A.B., U.S. ten Brink, P. Buhl, and T.M. Brocher, A multichannel seismic study of lithospheric flexure across the Hawaiian-Emperor seamount chain, *Nature, 315*, 105-111, 1985.

Wedgeworth, B.S., Ita Mai Tai Guyot: A comparative geophysical study of western Pacific seamounts, M.S. thesis, 90 pp., Univ. Hawaii, 1985.

Wedgeworth, B.S., and J.N. Kellogg, A 3-D gravity-tectonic study of Ita Mai Tai Guyot, an uncompensated seamount in the East Mariana Basin, this volume.

Williams, H., Geology of Tahiti, Moorea, and Maiao, *Bishop Museum Bull., 105*, 3-74, 1933.

Woollard, G.P., The interrelationships of crustal and upper mantle parameter values in the Pacific, *Rev. Geophys. Space Phys., 13*, 87-137, 1975.

Zucca, J.J., D.P. Hill, and R.L. Kovach, Crustal structure of Mauna Loa volcano, Hawaii, from seismic refraction and gravity data, *Bull. Seism. Soc. Amer., 72*, 1535-1550, 1982.